Journal of Applied Pharmaceutical Science Vol. 13(09), pp 095-105, September, 2023
Available online at http://www.japsonline.com
DOI: 10.7324/JAPS.2023.125985
ISSN 2231-3354

Prospective pulmonary drug delivery system of pirfenidone microparticles for pulmonary fibrosis

Uqie Shabrina Hasyyati[1], Silvia Surini[1*], Gatot Suhariyono Suhariyono[2]

[1]Laboratory of Pharmaceutics and Pharmaceutical Technology, Faculty of Pharmacy, Universitas Indonesia, Depok, Indonesia.
[2]Nuclear Metrology and Quality Safety Technology Research Center - Nuclear Power Research Organization, National Research and Innovation Agency, Tangerang Selatan, Indonesia.

ARTICLE INFO

Received on: 30/03/2023
Accepted on: 27/06/2023
Available Online: 04/09/2023

Key words:
Pirfenidone, pulmonary delivery, pulmonary fibrosis, microparticle, cytotoxicity study.

ABSTRACT

Orally administered pirfenidone in pulmonary fibrosis therapy induces numerous systemic adverse effects. This study aims to develop pirfenidone microparticles for pulmonary delivery to reduce the systemic adverse effects of pirfenidone. Ten formulations of pirfenidone microparticles were prepared using the spray drying method, including sodium carboxymethyl cellulose and sodium alginate as polymers, ammonium bicarbonate as porogen, and L-leucine as dispersing agent. These microparticles were evaluated using physicochemical characterization, stability, and *in vitro* cytotoxicity studies. The F10 formulation, which consisted of sodium alginate 1.0%, ammonium bicarbonate 0.3%, and L-leucine 0.4%, had the most relevant results for inhalation. The mass median aerodynamic diameters (MMADs) of F10 were 0.065, 0.597, 2.212, and 5.626 µm, ideal for deposition in the bronchiolar to the alveolar region. The stability study showed that the pirfenidone contents were 99.08%–100.00% and 98.83%–100.00%, with an increasing MMAD up to 5.895 and 6.273 µm at 30°C ± 2°C and 40°C ± 2°C, respectively. The *in vitro* cytotoxicity study revealed that the pulmonary epithelial cells (A549 cells) were less sensitive to the excipients in the formulation than pirfenidone ($p = 0.018$). Furthermore, F10 caused significantly lower interleukin-6 release than pirfenidone ($p < 0.05$). In conclusion, F10 shows suitable characteristics for pulmonary pirfenidone delivery in pulmonary fibrosis therapy.

INTRODUCTION

Pirfenidone, an anti-inflammation, antioxidant, and antifibrotic drug, is used in treating pulmonary fibrosis, such as idiopathic pulmonary fibrosis (IPF) (Canestaro *et al*., 2016). IPF is a progressive, chronic, age-related interstitial lung disease. It is expected to increase as the population ages, with an average untreated life expectancy of 3–5 years after diagnosis (Spagnolo *et al*., 2021). Pirfenidone has also been studied in clinical trials to treat post-COVID-19 pulmonary fibrosis (Bazdyrev *et al*., 2021), reported in patients with severe and moderate COVID-19 based on artificial intelligence analysis (Halawa *et al*., 2021). A meta-analysis study concluded that about 44.9% of COVID-19 survivors appear to have developed pulmonary fibrosis, which may mainly persist over time (Hama Amin *et al*., 2022). Fibrosis causes stiffness in the walls of the alveolus, which reduces the lungs' functional capacity and disrupts the respiratory process. A persistent decline in lung function can be fatal (Martinez *et al*., 2017; Spagnolo *et al*., 2021).

In the current treatment of pulmonary fibrosis, pirfenidone is taken orally in high doses (up to 2,403 mg/day) (Sayf, 2021). However, this route could lead to therapeutic discontinuation due to systemic adverse effects, including photosensitivity, gastrointestinal problems, anorexia, tiredness, and dizziness (Lancaster *et al*., 2017). Consequently, numerous studies have been conducted to identify an alternative route for pirfenidone administration. Delivering pirfenidone to the lungs through pulmonary delivery could reduce systemic exposure and subsequently reduce its adverse effect (Khoo *et al*., 2020). Pulmonary delivery also offers other benefits, such as reducing drug doses, duration, and the cost of the therapy (Putri *et al*., 2022).

**Corresponding Author*
Silvia Surini, Laboratory of Pharmaceutics and Pharmaceutical Technology, Faculty of Pharmacy, Universitas Indonesia, Depok, Indonesia.
E-mail: silvia @ farmasi.ui.ac.id

In this study, pirfenidone was designed to be delivered in solid microparticles due to better stability under storage conditions (Putri *et al*., 2022). Pirfenidone microparticles should have an aerodynamic diameter of 1–5 µm to be deposited in the bronchiolar to the alveolar region where the pulmonary fibrosis occurs. Particles should not be larger than 5 µm because they would deposit in the upper respiratory tract or smaller than 0.5 µm as they would be exhaled during exhalation (Chaurasiya and Zhao, 2020). The spray drying method offers the best approach to obtaining microparticles with an aerodynamic diameter of 1–5 µm. It produces controlled and reproducible particles with specific physicochemical properties by modifying the process parameters and particle formulation (Gallo and Bucalá, 2019).

Excipients used in pulmonary delivery should be nontoxic to the lungs, facilitate drug preparation and delivery, and prevent drug degradation (Surini *et al*., 2019). Sodium carboxymethyl cellulose (Na CMC) and sodium alginate (Na Ag) were generally recognized as safe polymers and are extensively studied as drug carriers in microparticles for inhalation. Therefore, Na CMC and Na Ag were used in this study. Previous studies revealed that Na CMC could improve the aerosolization efficiency of microparticles, prolong drug residence time due to its mucoadhesive properties, decrease mucociliary clearance, and increase drug absorption across pulmonary epithelia (Gallo and Bucalá, 2019; Xu *et al*., 2014). A combination of Na CMC and Na Ag produced inhalable hydrogel microparticles with a prolonged elimination half-life (Shahin *et al*., 2019). Ammonium bicarbonate was added to the formulation as porogen, and it had a blowing effect that could produce large particles with a small aerodynamic diameter (Ni *et al*., 2017). L-leucine was also added as a dispersing agent. It reduces interparticle force, thus decreasing cohesiveness and increasing the dispersibility of the microparticles (Alhajj *et al*., 2021).

This study aimed to develop pirfenidone microparticles for pulmonary delivery to target pulmonary fibrosis. The pirfenidone microparticles consisting of Na CMC and Na Ag, ammonium bicarbonate, and L-leucine were prepared using the spray drying method. The obtained microparticles were physically and chemically evaluated. A stability study was also conducted at 30°C ± 2°C and 40°C ± 2°C. Furthermore, an *in vitro* cytotoxicity study against the pulmonary epithelial cells (A549 cells) was also performed to assess the microparticles' safety.

MATERIALS AND METHODS

Materials

Materials used in this study were pirfenidone and L-leucine (Accela Chembio, China), Na CMC (Shandong Head, China), Na Ag (Shandong Jiejing, China), ammonium bicarbonate (PT. Smart Lab, Indonesia), and other chemicals of analytical grade.

Methods

Preparation of pirfenidone microparticles

Pirfenidone microparticles were prepared using the spray drying method with a B-290 Mini Spray Dryer with a 0.7 mm nozzle size (BÜCHI, Germany). The formulations are presented in Table 1. Na CMC and Na Ag, pirfenidone, and L-leucine were dissolved separately in sufficient water. Moreover, Na CMC and Na Ag were dissolved by stirring in hot water (70°C ± 5°C) until completely swelled, hydrated, and the solution was cooled down to room temperature (25°C ± 2°C). The solution of pirfenidone and L-leucine was then added, followed by ammonium bicarbonate powder for a maximum of 5 minutes before spray drying (Chvatal *et al*., 2019). The final solutions were then tested for viscosity using a rotational viscometer (Cole-Parmer, USA).

All formulations were spray-dried at 110°C of inlet temperature, 100% of aspiration (35 m^3/hour), 15% (2–5 ml/minute) of solution feed rate, and 44 mm spray airflow rate. The final spray-dried powders were collected, weighed, and preheated in the oven at 55°C ± 5°C until a moisture content of 3%–5% was obtained. The % process yield was calculated by dividing the amount of the powder collected by the solid content in the feed solution (Surini and Khotima, 2020). All microparticles were then stored in a desiccator at room temperature.

Microparticles morphology

The morphology of the microparticles was observed using a scanning electron microscope (JEOL JSM-IT200, JEOL, Japan). Microparticles were spread on the surface of the sample holder and then coated with gold particles using a fine particle coater. The morphology was visualized under 3.000–10.000× magnification (Surini *et al*., 2018).

Drug content (DC) and entrapment efficiency (EE)

The pirfenidone content in the microparticles was evaluated by dissolving the pirfenidone microparticles, equivalent to 10 mg of pirfenidone, in a phosphate buffer at a pH of 7.4 (Pardeshi *et al*., 2020). The sample solution was diluted and analyzed using a spectrophotometer at 311 nm (UV-Vis 1900i, Shimadzu, Japan). DC and EE were evaluated in triplicate and calculated using the following equation:

$$DC = \frac{\text{The actual pirfenidone content in the microparticles (mg)}}{\text{The microparticles weight (g)}}.$$

$$EE = \frac{\text{The actual pirfenidone content in the microparticles (mg)}}{\text{The theoretical pirfenidone content in the formulation (mg)}} \times 100\%.$$

Table 1. Formulation of pirfenidone microparticles.

Formulation	Composition (g/100 ml)				
	Pirfenidone	Na CMC	Na Ag	Ammonium bicarbonate	L-leucine
F1	0.1	1.0	0.0	0.2	0.4
F2	0.1	1.0	0.0	0.3	0.4
F3	0.1	0.5	0.5	0.2	0.4
F4	0.1	0.5	0.5	0.3	0.4
F5	0.1	0.7	0.3	0.2	0.4
F6	0.1	0.7	0.3	0.3	0.4
F7	0.1	0.3	0.7	0.2	0.4
F8	0.1	0.3	0.7	0.3	0.4
F9	0.1	0.0	1.0	0.2	0.4
F10	0.1	0.0	1.0	0.3	0.4

In vitro drug release study

An *in vitro* drug release study was performed in two dissolution mediums: a solution of phosphate buffer with sodium dodecyl sulfate 0.05% at pH 7.4 as a simulated lung fluid and a solution of potassium hydrogen phthalate 0.02 M at pH 4.5 as a simulated macrophage fluid (Surini *et al*., 2019). The pirfenidone microparticles equivalent to 5 mg of pirfenidone were put in 30 ml of dissolution media (Olsson *et al*., 2011). During the dissolution study, all samples were maintained at 37°C ± 1°C with a stirring speed of 100 rpm. Then, 6 ml of the sample was withdrawn at predetermined intervals of 15, 30, 60, 90, 120, 180, and 240 minutes, and the same volume of fresh buffer was added to the dissolution chamber. The samples were filtered using a 0.45 µm filter and measured at 311 nm (Pardeshi *et al*., 2020) using a spectrophotometer (UV-Vis 1900i, Shimadzu, Japan).

Microparticles density

The density of microparticles was represented by the tapped density (Ungaro *et al*., 2010) and was measured using tapped density tester (Erweka, Germany). Microparticles were loaded into a 5 ml cylindrical container. The volume of the microparticles was recorded after 1,250 taps. The tapped density was calculated using the following equation:

$$\text{Tapped density} = \frac{\text{Microparticles weight (g)}}{\text{Microparticles volume after 1,250 taps (ml)}}.$$

Microparticles size

The geometric particle size was measured using a particle size analyzer (Beckman Coulter LS 100Q, Beckman Coulter, USA). Moreover, the aerodynamic particle size was analyzed using a cascade impactor (Andersen, Japan) and expressed as median aerodynamic diameter (MMAD), obtained from impactor data processing software (Diaz *et al*., 2015).

Stability study

A stability study of pirfenidone microparticles was conducted at 30°C ± 2°C and 40°C ± 2°C. The evaluation was performed at the initial study and at the 6th, 12th, and 24th weeks for the DC in the pirfenidone microparticles. The MMAD was also evaluated at the initial study and the 6th and 12th weeks of storage.

In vitro cytotoxicity study

Cytotoxicity of microparticles was studied against the human pulmonary epithelial cells (A549 cells). Cells were suspended in RPMI-1640 medium supplemented with fetal bovine serum and penicillin-streptomycin. Cells were incubated for 24 hours at 37°C and CO_2 5%. Samples used in this study were nonmedicated microparticles (excipients), pirfenidone, and the chosen formulation. Each sample was added in triplicate, and samples and the cells were then incubated for 24 hours. Afterward, 3-[4,5-dimethylthiazol-2-yl]-2,5 diphenyl tetrazolium bromide (MTT) was added to the well, and the incubation was continued for 4 hours. Ethanol 70% was added to the well before measuring the optical density (OD) at 595 nm using a microplate reader. The viable cells were calculated using the following equation:

$$\text{\% cell viability} = \frac{\text{OD of samples}}{\text{OD of control}} \times 100\%.$$

Pirfenidone and the chosen formulation were further studied to observe their impact on releasing the proinflammatory cytokine, namely, interleukin-6 (IL-6), from the A549 cell line. There were two concentrations used in this study: the first concentration was below the inhibitory concentration at 50% (IC_{50}); the second was equivalent to the IC_{50} from the MTT results. The samples and the A549 cells were incubated for 24 hours at 37°C with 5% CO_2. Then, the cells were lysed before being centrifuged to collect the supernatant. The samples were prepared following the supplier's protocol for the human IL-6 ELISA kit. A microplate reader was used to measure the color intensity at 450 nm. The concentrations of IL-6 in each sample were calculated by interpolation from the standard curve (MilliporeSigma, 2018).

Statistical analysis

Statistical analysis in IBM Statistical Package for the Social Sciences Statistic 22 was performed to determine the significant differences between samples using a *t*-test for normally distributed data and Mann–Whitney for non-normally distributed data. A p value of <0.05 was considered significant.

RESULTS AND DISCUSSION

Preparation of pirfenidone microparticles

Before starting the spray drying process, the viscosity of the formulation was measured to ensure that all formulations were feasible to be sprayed. Theoretically, the higher the solid content in the formulations' solution, the higher the viscosity of the solution. Therefore, only formulations with the higher solid content, which was 1.8%, were measured for viscosity: F2, F4, F6, F8, and F10. Those formulations showed a viscosity below 400 cps, as shown in Table 2. Thus, all the pirfenidone microparticle formulations could be processed by spray drying.

The spray drying method produced fine white powder microparticles, as illustrated in Figure 1. The process yield ranged from 53.30% to 60.00%. Based on Table 2, an inverse correlation was observed between viscosity and process yield. The process yield was significantly higher in the formulations with a single polymer than that in the formulations with two kinds of polymers (p = 0.001). The viscosity of the formulations influenced the atomization process, which impacted the size of droplets and drying time. The higher the viscosity, the larger the droplet size. As a result, a longer drying time was required. Droplets that were not completely dry would adhere to the walls of the drying chamber, forming a wet mass and lowering the process yield (Alhajj *et al*., 2021; Esposito *et al*., 2020). A higher process yield could be obtained by increasing the batch and spray dryer sizes, which had higher process efficiency (Gawałek, 2021; Nekkanti *et al*., 2009).

Pirfenidone microparticles had a moisture content between 6.26% and 8.74% after spray drying, as shown in Table 3. Formulation with Na Ag had the highest moisture content due to the higher hygroscopicity of Na Ag compared to Na CMC. The drying process was continued until a moisture content of 3%–5% to achieve better formulation stability. The reduction of moisture content could also lead to the reduction of particle density, thus

Table 2. The viscosity and process yield of pirfenidone microparticle formulations.

Formulation	Viscosity (cps)[a]	Process yield (%)
F1	NA	57.30
F2	202.87 ± 1.78	58.70
F3	NA	53.30
F4	222.3 ± 1.61	53.30
F5	NA	53.30
F6	222.83 ± 1.61	55.00
F7	NA	55.00
F8	237.40 ± 0.92	55.60
F9	NA	57.30
F10	207.97 ± 0.87	60.00

NA: Not analyzed.
[a]Values are represented as mean ± standard deviation (n = 3).

Figure 1. The physical appearance of pirfenidone microparticles: Formulation 1 (F1) to Formulation 10 (F10).

enhancing the particles' aerosolization performance (Shahin *et al*., 2019).

Microparticles morphology

As presented in Figure 2, pirfenidone microparticles exhibited wrinkled raisin-like surfaces and dented microparticles. No significant differences were observed on microparticles with different drug carriers, such as Na CMC in Figure 2A, the combination of Na CMC and Na Ag in Figure 2B, and Na Ag in Figure 2D. The different concentrations of ammonium bicarbonate, as in Figure 2C (0.2%) and 2D (0.3%), also did not cause significant differences in the morphology of the particles. Generally, polysaccharide microparticles have wrinkled surfaces due to the rapid loss of water molecules bound to the hydrophilic polymer during drying at high temperatures (Gallo *et al*., 2017; Surini *et al*., 2009).

L-leucine was added to the formulation as dispersing agent. It improves microparticle aerosolization by reducing hygroscopicity, increasing dispersibility, or altering the microparticle surface morphology (Wang *et al*., 2021). The addition of L-leucine to the formulations increased the surface roughness, resulting in more dented or crumpled microparticles than those in the formulation without L-leucine, as in Figure 2E (Chvatal *et al*., 2019). Those irregular shape microparticles had lower interparticle force and thus exhibited better aerodynamic properties than smooth and spherical microparticles (Alhajj *et al*., 2021). L-leucine, a nonpolar aliphatic amino acid with surface-active characteristics in aqueous solutions, will likely accumulate at an air-solvent interface (Simon *et al*., 2016). It quickly reached supersaturation during drying and would solidify before the droplet thoroughly dried, forming low-density hollow particles (Alhajj *et al*., 2021). L-leucine on the droplet surface could not flow as rapidly as the particle shrinks when the solvent evaporated (Péclet number > 1); hence, the L-leucine surface layer collapsed, resulting in dented or crumpled particles. The degree of the crumpled particles was determined by the L-leucine mass fraction in the formulation (Simon *et al*., 2016).

Table 3. Moisture content of pirfenidone microparticles.

Formulation	Moisture content (%)	
	After spray drying	After heating in the oven (55°C ± 5°C)
F1	6.45	4.41
F2	6.95	4.43
F3	6.57	3.84
F4	6.83	3.59
F5	6.26	4.34
F6	6.65	4.52
F7	7.22	4.62
F8	7.18	4.49
F9	8.09	4.82
F10	8.74	4.82

DC and EE

DC calculated pirfenidone concentration on the powder, while EE calculated the actual percentage of pirfenidone loaded within microparticles compared to the initial one. Pirfenidone microparticles had DC ranging from 51.76 to 58.97 mg/g microparticles and EE of 77.64%–88.46%. Based on Table 4, the trend suggested that Na CMC had positive values on DC and EE. Formulation with Na CMC (F1 and F2) had significantly higher DC than the formulation with Na Ag (F9 and F10), with p values of <0.001 and 0.001, respectively. A similar trend was also observed in the EE. F1 had significantly higher EE than F9 ($p < 0.001$), and so did F2 than F10 ($p = 0.001$).

In the spray drying process, the solvent evaporation rate determined the drug entrapment within the polymeric particles. The drying process was faster in the formulations with Na CMC than those with Na Ag. This was indicated by the lower moisture content after spray drying in the formulations with Na CMC than that in the formulations with Na Ag, as shown in Table 3. During solvent evaporation, the droplets would shrink and subsequently dictate the arrangement of the solutes on the surface and the center of the particles. The faster the drying process, the faster the polymer precipitation, which limited drug diffusion across the phase boundary, thus increasing the EE (Mishra and Mishra, 2011; Shahin *et al*., 2019).

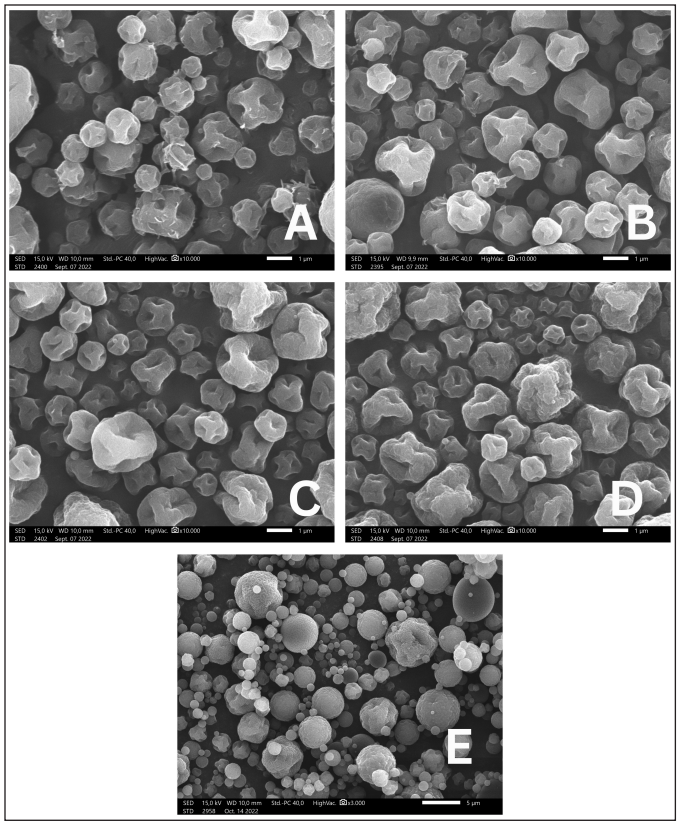

Figure 2. Morphology of pirfenidone microparticles: Formulation 2 (A), Formulation 4 (B), Formulation 9 (C), Formulation 10 (D), formulation without L-leucine (E) (A–D: 10.000× magnification, E: 3.000× magnification).

Table 4. DC and EE of pirfenidone microparticles.

Formulation	DC (mg/g microparticles)	EE (%)
F1	58.97 ± 0.27	88.46 ± 0.41
F2	58.04 ± 0.13	87.06 ± 0.19
F3	53.56 ± 0.11	80.34 ± 0.17
F4	53.61 ± 0.11	80.42 ± 0.16
F5	53.72 ± 0.29	80.58 ± 0.43
F6	55.17 ± 0.31	82.76 ± 0.47
F7	53.60 ± 0.39	80.40 ± 0.58
F8	53.50 ± 0.29	80.25 ± 0.43
F9	51.76 ± 0.17	77.64 ± 0.25
F10	53.90 ± 0.23	80.85 ± 0.34

All values are represented as mean ± standard deviation (n = 3).

In vitro drug release study

Figures 3 and 4 present the dissolution profile of pirfenidone microparticles. Pirfenidone had a higher dissolution rate in the simulated lung fluid (94.33% ± 0.43% in 90 minutes) than in the simulated macrophage fluid (79.79% ± 1.51% in 90 minutes). This is attributed to the higher solubility of pirfenidone in the simulated lung fluid (±8.8 mg/ml) than that in the simulated macrophage fluid (±8.6 mg/ml). Furthermore, the addition of sodium dodecyl sulfate in the simulated lung fluid could increase pirfenidone solubility. The dissolution profile of pirfenidone differed from that of pirfenidone microparticles in both mediums ($p < 0.05$), which was due to the presence of excipients in the microparticles.

In the 120-minute study, all formulations of pirfenidone microparticles had reached a cumulative release of 80% or more in both dissolution mediums. It indicated that high pirfenidone concentrations were available within 120 minutes from all formulations. In lung parenchyma, pirfenidone inhibits transforming growth factor -β, produced by various cells during epithelial damage. Pirfenidone also reduces the number of alveolar macrophages and the macrophage inflammatory activity induced by cytokines like IL-1, tumor necrosis factor, and platelet-derived growth factor (Ruwanpura *et al*., 2020).

Microparticles density

The densities of pirfenidone microparticles are presented in Table 5. Pirfenidone microparticles had a density of 0.308–0.373 g/ml. This indicates that pirfenidone microparticles had low mass density. Those particles had good aerodynamic properties, making them suitable for pulmonary delivery. A study showed that relatively large particles with a diameter of more than 5 µm and low mass density (<0.4 g/cm^3) can be successfully inspired into the lungs and have excellent aerosolization properties (Shahin *et al*., 2021).

Microparticles size

Pirfenidone microparticles had a median geometric particle size ranging from 2.761 to 4.172 µm with a span value of more than 1.5, which indicated large particle size distribution (Shahin *et al*., 2019). Pirfenidone microparticles mainly consisted of microparticles ranging from 1 to 5 µm ($p < 0.001$), as shown in Table 6. Particle size affected the deposition site of microparticles in the lung. Microparticles with a diameter smaller than 5 µm could deposit in the bronchiolar to the alveolar regions (Chaurasiya and Zhao, 2020). Thus, pirfenidone microparticles were predicted to be deposited mainly in those regions.

However, even though particles of 1–3 µm size were deposited maximally in the alveolar region, they were prone to be engulfed faster by alveolar macrophages. Phagocytosis diminished with increasing particle size beyond 2–3 µm (Edwards *et al*., 1998). Another study revealed that maximal phagocytosis took place when the particle size was in the range of 1.0–2.0 µm. Macrophages appear to be able to distinguish the size of foreign materials adhering to them (Tabata and Ikada, 1988). The phagocytosis depended greatly on the particle size and the number of particles. A study showed that the population of rat alveolar macrophages that phagocytosed 1 or 3 µm rifampicin-loaded poly(lactic-co-glycolic) acid (PLGA) particles was larger than that of those phagocytosed 6 or 10 µm particles. This is likely due to the limited size of macrophages (around 15 µm) that will phagocytose more particles that are smaller in size (Hirota *et al*., 2007).

Based on the previous description, 1–3 µm pirfenidone microparticles were also prone to be engulfed faster to some extent. However, Na CMC and Na Ag were hydrophilic polymers that could swell when encountered with liquid. A study showed

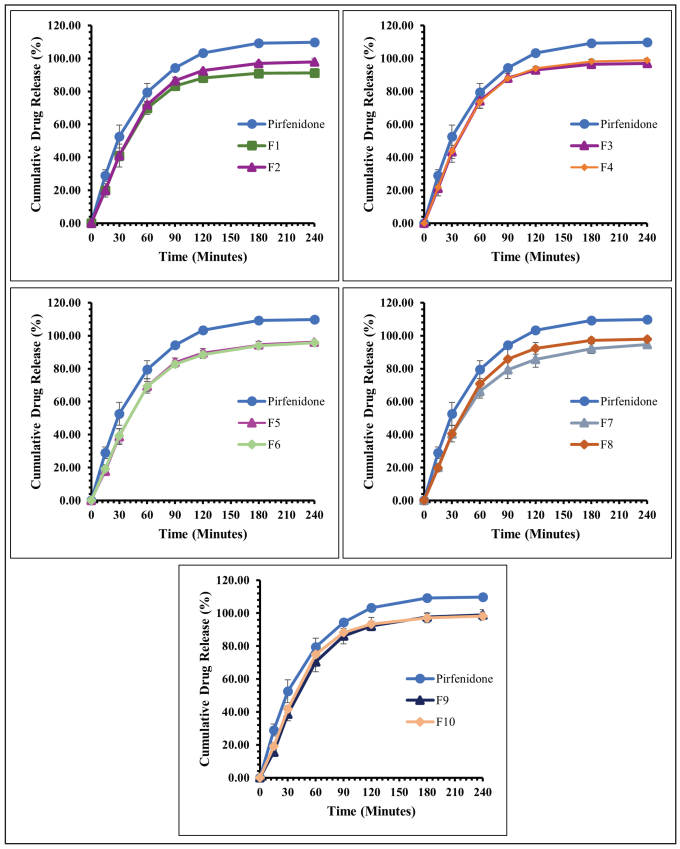

Figure 3. The dissolution profile of pirfenidone microparticles in phosphate buffer and sodium dodecyl sulfate 0.05% (pH 7.4): Formulation 1 (F1) to Formulation 10 (F10). All values are presented as mean ± standard deviation ($n = 3$).

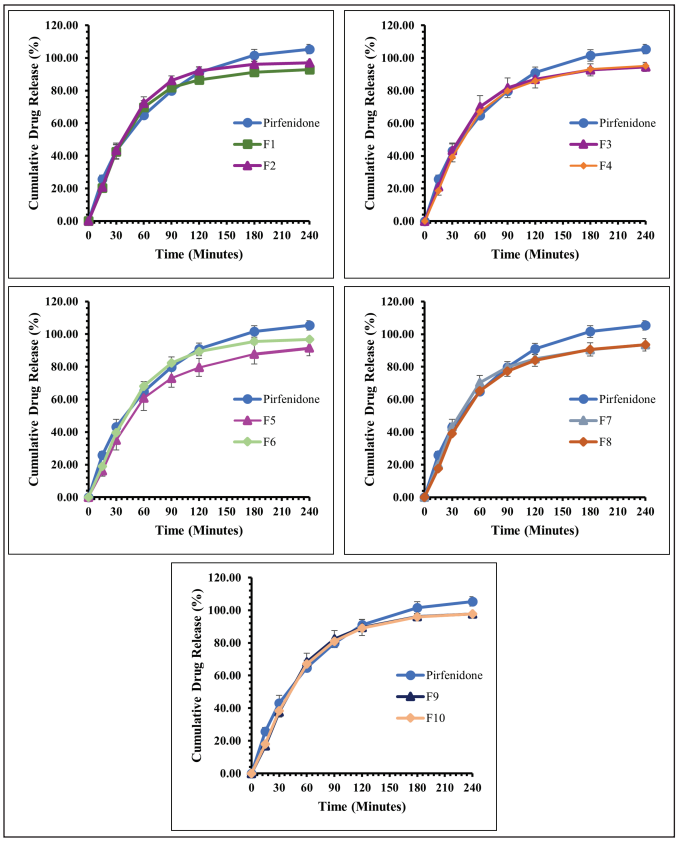

Figure 4. The dissolution profile of pirfenidone microparticles in potassium hydrogen phthalate 0.02 M (pH 4.5): Formulation 1 (F1) to Formulation 10 (F10). All values are presented as mean ± standard deviation ($n = 3$).

that microparticles formulated with Na CMC and Na Ag could swell up to six times their original weight during the first hour of incubation with the simulation lung fluid. This rapid increase in size was expected to reduce uptake by alveolar macrophages and significantly increase the residence time of microparticles in the lung (Shahin *et al.*, 2019). As a result, all pirfenidone microparticle formulations had the potency to deposit in the lung and to be engulfed slower by alveolar macrophages.

Table 7 shows the aerodynamic diameter of pirfenidone microparticles. The aerodynamic diameter was a fundamental factor in determining particle deposition in the lungs. It considered factors such as apparent particle density and dynamic particle shape that affect the aerosolization of particles during inhalation (Yoshida *et al.*, 2020). Aerodynamic diameter is presented as MMAD, defined as the diameter at the midpoint of microparticle frequency distribution where 50% of particles were larger and 50% of particles were smaller than the stated diameter value of MMAD (Mahmoud *et al.*, 2018). Pirfenidone microparticles had multimodal distribution indicated by more than one value of MMAD. It illustrated the polydispersity and broad particle size distribution that were reflected in the particle deposition profiles in the cascade impactor stages.

Pirfenidone microparticles had an MMAD ranging from 0.055 to 12.417 µm with a geometric standard deviation (GSD) of 1.259–3.981. They were mainly distributed in stages

Table 5. The density of pirfenidone microparticles.

Formulation	Particles' density (g/ ml)
F1	0.339 ± 1.695
F2	0.339 ± 1.695
F3	0.364 ± 1.818
F4	0.345 ± 1.195
F5	0.370 ± 1.852
F6	0.313 ± 1.563
F7	0.313 ± 1.563
F8	0.308 ± 1.539
F9	0.351 ± 1.755
F10	0.373 ± 1.083

All values are represented as mean ± percentage relative standard deviation ($n = 3$).

0–2 of the cascade impactor ($p < 0.001$). Particles trapped in those stages ranged in size from 4.7 to 14 µm. Meanwhile, around 19.20%–43.95% were trapped on stage 3 to filter (0.01–4.7 µm). Microparticles with an MMAD of more than 6 µm would deposit in the tracheal region due to inertial impaction. Meanwhile, microparticles with an MMAD around 2–5 µm would deposit in the bronchiolar region due to sedimentation. Smaller microparticles less than 2 µm would deposit in the alveolar region due to diffusion (Chaurasiya and Zhao, 2020).

Table 6. Geometric diameter of pirfenidone microparticles.

Formulation	Particle size (µm)			Span	Particle size distribution (%)	
	Dv10%	Dv50%	Dv90%		1 to less than 5 µm	5 to less than 10 µm
F1	1.277	3.682	7.810	1.774	61.65	31.37
F2	1.244	3.725	7.491	1.677	62.12	30.08
F3	0.904	3.472	7.843	1.999	56.70	29.03
F4	1.197	3.278	7.184	1.826	67.36	24.45
F5	1.071	4.172	8.870	1.869	51.46	35.41
F6	1.140	3.889	8.296	1.840	56.89	31.84
F7	1.013	3.106	6.819	1.869	66.75	21.67
F8	1.008	2.854	6.586	1.954	69.56	18.76
F9	0.956	2.761	6.300	1.936	70.02	17.33
F10	1.030	2.832	6.540	1.946	69.11	15.18

Among those formulations, F10 showed the smallest MMADs, which were 0.065, 0.597, 2.212, and 5.626 µm. Furthermore, the mass distribution in stage 3 to filter was higher than that of other formulations. It was predicted that F10 microparticles would deposit more in the bronchial to the alveolar region than those in the other formulations with larger MMADs. An *in vivo* study of pirfenidone respirable powder with bigger particle size, geometric size of 7 µm, which is mainly distributed in cascade impactor stages 0 and 1, showed suppressing antigen-evoked pulmonary inflammation in male Sprague–Dawley rats after intratracheal insufflation. It also had 90–130-fold less exposure to the skin and eye compared to the oral phototoxic pirfenidone dose (Onoue *et al*., 2013). These data showed that F10 had the potency to be delivered to the lower airway region, reduced pirfenidone systemic exposure, and suppressed inflammation in the lung tissue despite having the largest MMAD of 5.626 µm. Thus, F10 was selected as the lead formulation.

The effect of ammonium bicarbonate concentration could be observed in F9 and F10, which used Na Ag as the drug carrier. The addition of ammonium bicarbonate concentration decreased the MMAD but not the geometric diameter. The largest MMAD on F9 was 10.740 µm; meanwhile, the largest MMAD on F10 was 5.626 µm. The decomposition of ammonium bicarbonate during drying caused the droplets to enlarge and lose density. Consequently, microparticles possessed greater geometric diameters but smaller aerodynamic diameters (Ni *et al*., 2017). However, this effect could not be seen in other formulations, possibly due to the low variability in ammonium bicarbonate concentration and the error associated with individual measurements, which could influence these outcomes.

Stability study

The stability study was conducted on F10 as the lead formulation. There were no significant changes in pirfenidone content during the stability study (week 0 *vs.* week 24) at room temperature ($p = 0.161$) and accelerated conditions ($p = 0.079$), as shown in Table 8. The pirfenidone content ranged from 100.00% to 99.08% at room temperature (30°C ± 2°C) and 100.00% to 98.83% at accelerated conditions (40°C ± 2°C). However, the MMADs results showed an increasing trend up to 5.895 and 6.273 µm at 30°C ± 2°C and 40°C ± 2°C, respectively. This might be due to the aggregation of microparticles. The over-dented microparticles could form mechanical interlocking between the particles, thus promoting particle aggregation (Wang *et al*., 2021).

***In vitro* cytotoxicity study**

The human epithelial cell line (the A549 cells) was incubated with nonmedicated microparticles (excipients), pirfenidone, and pirfenidone microparticles (F10). F10 was precisely weighted, equivalent to the pirfenidone concentration used in this study. The powder concentration of F10 was 0–18,500 µg/ ml. As illustrated in Figure 5, the cell viability decreased as the concentration of nonmedicated microparticles increased. The nonmedicated microparticles swelled and absorbed the culture media, negatively impacting cell viability (Shahin *et al*., 2019). Moreover, when dissolved in the growth medium, the nonmedicated microparticles formed a viscous solution that hindered the cells' attachment to the well during cell division time, thus lowering the cells' viability (Chary *et al*., 2022). A similar trend was also observed when cells were incubated with different pirfenidone concentrations. The A549 cell viability decreased with increasing the concentration of pirfenidone. The decrease of the A549 cells' viability was significantly lower when incubated with nonmedicated microparticles than that incubated with pirfenidone at a sample concentration of up to 1,000 µg/ml ($p = 0.018$). This indicated that the A549 cell was less sensitive to the nonmedicated microparticles (excipients) than pirfenidone.

Cell viability decreased when incubated with F10 due to the accumulation of nonmedicated microparticles (excipients) and pirfenidone effects on the A549 cells. As the F10 concentration increased, the cell viability decreased significantly compared to that of the nonmedicated microparticles at a sample concentration of up to 1,000 µg/ml ($p < 0.001$). Compared to pirfenidone, the cells' viability decreased significantly at a sample concentration of up to 125 µg/ml ($p = 0.001$). Based on the cell viability data, the IC_{50} of the samples was then calculated. The results showed that the IC_{50} of nonmedicated microparticles (excipients), pirfenidone, and F10 were 1,185.63, 685.76, and 437.58 µg/ml, respectively.

The impacts of pirfenidone and F10 on releasing proinflammatory cytokines, namely, IL-6, were also studied. IL-6 is a proinflammatory cytokine that increases the number and activity of immune cells, such as leukocytes and neutrophils, in the lung area. It was secreted as part of the immune system to eliminate foreign materials that entered the lung, including microparticles.

Table 7. Aerodynamic diameter of pirfenidone microparticles.

Formulation	Particle size		Mass distribution in ACI (%)	
	MMAD (µm)	GSD	Stages 0 to 2	Stage 3 to filter
F1	2.208	3.219	75.79%	24.21%
	2.632	1.391		
	8.145	1.723		
F2	0.601	1.399	77.51%	22.49%
	6.343	1.695		
	10.889	1.279		
F3	0.655	1.502	70.62%	29.32%
	3.642	1.286		
	9.243	1.707		
F4	0.609	1.351	80.80%	19.20%
	1.580	2.319		
	7.725	1.700		
F5	0.459	1.407	76.81%	23.19%
	1.710	1.261		
	4.924	1.413		
	12.417	1.263		
F6	2.729	1.784	80.73%	19.27%
	4.523	1.302		
	11.695	1.391		
F7	0.055	2.398	65.14%	34.86%
	1.072	2.257		
	4.484	2.062		
	11.508	1.259		
F8	0.406	1.360	59.55%	40.45%
	1.889	1.260		
	4.022	1.326		
	10.593	1.581		
F9	0.448	1.280	57.44%	42.56%
	1.591	1.260		
	4.004	1.354		
	10.740	1.608		
F10	0.065	2.097	56.05%	43.95%
	0.597	1.259		
	2.212	3.981		
	5.626	1.863		

ACI: Andersen cascade impactor; MMAD: mass median aerodynamic diameter; GSD: geometric standard deviation.

Excessive activity of immune cells can cause damage to lung cells, which can lead to various diseases, including pulmonary fibrosis (Kim *et al*., 2017).

Based on the MTT results, pirfenidone concentrations used in this study were 300 and 690 µg/ml. Meanwhile, F10 concentration was calculated based on the pirfenidone content, which was 300 µg/ml (equivalent to 5,550 µg/ml powder) and 440 µg/ml (equivalent to 8,140 µg/ml powder). Figure 6 shows the IL-6 release from the A549 cells. The control cells released IL-6 at 8,057 ± 271 pg/ml for 24 hours. IL-6 has dual functions in cells, one of which is to prevent apoptosis in type 2 alveolar cells (She *et al*., 2021). The A549 cells have morphological and biochemical similarities with type 2 alveolar cells (Acosta *et al*., 2016), so releasing IL-6 from control cells was likely to prevent cell apoptosis.

The concentration of IL-6 released from the A549 cells was significantly lower when incubated with F10 than when incubated with pirfenidone at a sample concentration of 300 µg/ml ($p < 0.001$). A similar result was also obtained when cells were incubated with 690 µg/ml of pirfenidone and 440 µg/ml of F10 ($p = 0.004$). This indicates that A549 cells were less sensitive to F10 than pirfenidone. Moreover, compared to the control cells,

Table 8. Stability study of F10.

Time (week)	Storage condition	DC (%)[a]	Particle size	
			MMAD (µm)	GSD
Initial	-	100.00 ± 0.00	0.065	2.097
			0.597	1.259
			2.212	3.981
			5.626	1.863
6th	30°C ± 2°C	99.46 ± 0.42	0.054	1.595
			0.559	1.276
			0.733	1.454
			5.895	1.695
	40°C ± 2°C	99.80 ± 0.82	0.064	3.857
			0.660	1.391
			1.179	1.259
			6.273	1.747
12th	30°C ± 2°C	99.08 ± 0.28	0.634	1.328
			5.574	1.785
	40°C ± 2°C	98.97 ± 0.11	0.598	1.259
			0.728	1.387
			5.861	1.810
24th	30°C ± 2°C	99.24 ± 0.61	NA	NA
	40°C ± 2°C	98.83 ± 0.61	NA	NA

MMAD: mass median aerodynamic diameter; GSD: geometric standard deviation; NA: not analyzed.
[a]Values are represented as mean ± standard deviation (n = 3).

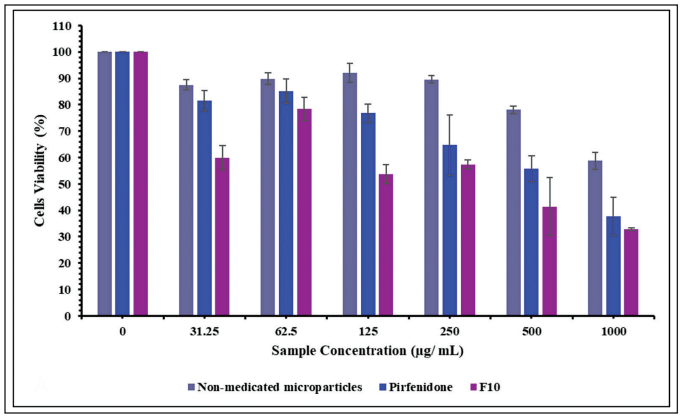

Figure 5. The A549 cell viability (%) after being exposed to nonmedicated microparticles, pirfenidone, and pirfenidone microparticles (F10). All values are presented as mean ± standard deviation (n = 3).

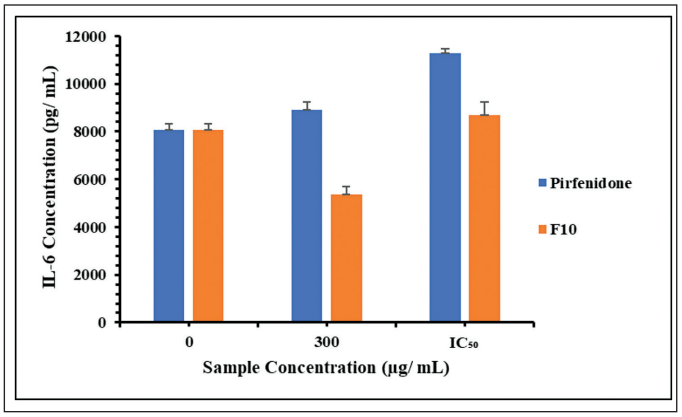

Figure 6. The IL-6 release concentration from the A549 cells after being exposed to pirfenidone and pirfenidone microparticles (F10). The IC_{50} was 690 µg/ ml and 440 µg/ ml for pirfenidone and F10, respectively.

F10 at a concentration of 300 µg/ml could inhibit the release of IL-6 from A549 cells, as indicated by significantly lower IL-6 release (p = 0.019). IL-6 plays a role in inducing macrophages into a hyperfibrotic phenotype, inducing fibroblast proliferation, and increasing collagen synthesis (She *et al*., 2021). Therefore, F10 also has the potential to reduce the progression of IPF. Further *in vivo* studies are warranted to assess the safety and efficacy of pirfenidone microparticles since *in vitro* toxicity studies could be affected by many factors. As a result, *in vitro* studies sometimes showed little correlation with *in vivo* studies (Sayes *et al*., 2007).

CONCLUSION

Pirfenidone microparticles prepared using the spray drying method have been developed for pulmonary delivery. The lead formulation of pirfenidone microparticles (F10) consisted of Na Ag 1.0%, ammonium bicarbonate 0.3%, and L-leucine 0.4%. F10 had an irregular shape and low density (0.373 ± 1.083% g/ml) with MMADs of 0.065, 0.597, 2.212, and 5.626 µm. Furthermore, F10 had the highest percentage of particles smaller than 4.7 µm. Those characteristics were ideal for deposition in the bronchiolar to the alveolar

regions. It had stable pirfenidone content for 24 weeks of storage at room temperature and accelerated conditions; however, the MMADs increased due to aggregation. The *in vitro* cytotoxicity study on the A549 cells showed that the excipients used in the formulation were considered safer for the cells than pirfenidone. Additionally, compared to pirfenidone, F10 caused significantly reduced the IL-6 release from the cells. In conclusion, F10 microparticles show appropriate characteristics for pulmonary drug delivery. They should be further investigated to explore their efficiency in treating pulmonary fibrosis.

ACKNOWLEDGMENTS

The authors gratefully acknowledge the Ministry of Education, Culture, Research, and Technology of Indonesia for financial support through the magister student research grant with contract number NKB-896/UN2.RST/HKP.05.00/2022.

AUTHORS' CONTRIBUTIONS

USH designed the study, conducted the laboratory experiment, analyzed and interpreted data, and wrote the manuscript. GS supervised the data analysis. Meanwhile, SS contributed to the study design, supervised the laboratory experiment and data analysis, revised the manuscript critically, and granted the final approval.

CONFLICTS OF INTEREST

The authors report no financial or other conflicts of interest in this work.

ETHICAL APPROVAL

This study does not involve any animal or human subjects.

DATA AVAILABILITY

All data generated and analyzed are included in this research article.

PUBLISHER'S NOTE

This journal remains neutral with regard to jurisdictional claims in published institutional affiliation.

REFERENCES

Acosta, MF, Muralidharan, P, Meenach, SA, Hayes, D, Black, SM, Mansour, HM. *In Vitro* pulmonary cell culture in pharmaceutical inhalation aerosol delivery: 2-D, 3-D, and *In Situ* bioimpactor models. Curr Pharm Des, 2016; 22(17):2522–31.

Alhajj N, O'Reilly NJ, Cathcart H. Designing enhanced spray dried particles for inhalation: A review of the impact of excipients and processing parameters on particle properties. Powder Technol, 2021; 384:313.

Bazdyrev E, Rusina P, Panova M, Novikov F, Grishagin I, Nebolsin V. Lung fibrosis after COVID-19: treatment prospects. Pharmaceuticals (Basel), 2021; 14(8):807.

Canestaro WJ, Forrester SH, Raghu G, Ho L, Devine BE. Drug treatment of idiopathic pulmonary fibrosis systematic review and network meta-analysis. Chest, 2016; 149(3):756–66.

Chary A, Groff K, Stucki AO, Contal S, Stoffels C, Cambier S, Sharma M, Gutleb AC, Clippinger AJ. Maximizing the relevance and reproducibility of A549 cell culture using FBS-free media. Toxicol Vitr, 2022; 83:105423.

Chaurasiya B, Zhao Y-Y. Dry powder for pulmonary delivery: a comprehensive review. Pharmaceutics, 2020; 13(1):31.

Chvatal A, Ambrus R, Party P, Katona G, Jójárt-Laczkovich O, Szabó-Révész P, Fattal E, Tsapis N. Formulation and comparison of spray dried non-porous and large porous particles containing meloxicam for pulmonary drug delivery. Int J Pharm, 2019; 559:68–75.

Diaz JMF, Brana MAR, Arganza B. A complete computer program to fit the data from an impactor to a sum of log normals. In: 7th International Aerosol Conference, St. Paul, MN, 2015.

Edwards DA, Ben-Jebria A, Langer R. Recent advances in pulmonary drug delivery using large, porous inhaled particles. J Appl Physiol, 1998; 85(2):379–85.

Esposito T, Mencherini T, Del Gaudio P, Auriemma G, Franceschelli S, Picerno P, Aquino RP, Sansone F. Design and development of spray-dried microsystems to improve technological and functional properties of bioactive compounds from hazelnut shells. Molecules, 2020; 25(6):1273.

Gallo L, Bucalá V. A review on influence of spray drying process parameters on the production of medicinal plant powders. Curr Drug Discov Technol, 2019; 16(4):340–54.

Gallo L, Bucalá V, Ramírez-Rigo MV. Formulation and characterization of polysaccharide microparticles for pulmonary delivery of sodium cromoglycate. AAPS PharmSciTech, 2017; 18(5):1634–45.

Gawałek J. Effect of spray dryer scale size on the properties of dried beetroot juice. Molecules, 2021; 26(21):6700.

Halawa S, Pullamsetti SS, Bangham CRM, Stenmark KR, Dorfmüller P, Frid MG, Butrous G, Morrell NW, de JP, Vinicio A, Stuart DI, O'Gallagher K, Shah AM, Aguib Y, Yacoub MH. Potential long-term effects of SARS-CoV-2 infection on the pulmonary vasculature: a global perspective. Nat Rev Cardiol, 2021:0123456789.

Hama Amin BJ, Kakamad FH, Ahmed GS, Ahmed SF, Abdulla BA, Mohammed SH, Mikael TM, Salih RQ, Ali Rk, Salh AM, Hussein DA. Post COVID-19 pulmonary fibrosis; a meta-analysis study. Ann Med Surg, 2022; 77:103590.

Hirota K, Hasegawa T, Hinata H, Ito F, Inagawa H, Kochi C, Soma GI, Makino K, Terada H. Optimum conditions for efficient phagocytosis of rifampicin-loaded PLGA microspheres by alveolar macrophages. J Control Release, 2007; 119(1):69–76.

Khoo JK, Bruce Montgomery A, Otto KL, Surber M, Faggian J, Lickliter JD, Glaspole I. A randomized, double-blinded, placebo-controlled, dose-escalation phase 1 study of aerosolized pirfenidone delivered via the PARI investigational eFlow nebulizer in volunteers and patients with idiopathic pulmonary fibrosis. J Aerosol Med Pulm Drug Deliv, 2020; 33(1):15–20.

Kim HR, Shin DY, Chung KH. *In vitro* inflammatory effects of polyhexamethylene biguanide through NF-κB activation in A549 cells. Toxicol Vitr, 2017; 38:1–7.

Lancaster LH, de Andrade JA, Zibrak JD, Padilla ML, Albera C, Nathan SD, Wijsenbeek MS, Stauffer JL, Kirchgaessler KU, Costabel U. Pirfenidone safety and adverse event management in idiopathic pulmonary fibrosis. Eur Respir Rev, 2017; 26(146):170057.

Mahmoud AA, Elkasabgy NA, Abdelkhalek AA. Design and characterization of emulsified spray dried alginate microparticles as a carrier for the dually acting drug roflumilast. Eur J Pharm Sci, 2018; 122:64–76.

Martinez FJ, Collard HR, Pardo A, Raghu G, Richeldi L, Selman M, Swigris JJ, Taniguchi H, Wells AU. Idiopathic pulmonary fibrosis. Nat Rev Dis Prim, 2017; 3:17074.

MilliporSigma. Certificate analysis of human IL-6 ELISA Kit. 2018. [Online]. Available via https://www.sigmaaldrich.com/ID/en/coa/SIGMA/RAB0307/0713I0141 (Accessed 19 October 2022).

Mishra M, Mishra B. Formulation optimization and characterization of spray dried microparticles for inhalation delivery of doxycycline hyclate. Yakugaku Zasshi, 2011; 131(12):1813–25.

Nekkanti V, Muniyappan T, Karatgi P, Hari MS, Marella S, Pillai R. Spray-drying process optimization for manufacture of drug–cyclodextrin complex powder using design of experiments. Drug Dev Ind Pharm, 2009; 35(10):1219–29.

Ni R, Muenster U, Zhao J, Zhang L, Becker-Pelster EM, Rosenbruch M, Mao S. Exploring polyvinylpyrrolidone in the engineering of large porous PLGA microparticles via single emulsion method with tunable sustained release in the lung: *in vitro* and *in vivo* characterization. J Control Release, 2017; 249:11–22.

Olsson B, Bondesson E, Borgström L, Edsbäcker S, Eirefelt S, Ekelund K, Gustavsson L, Hegelund MT. Pulmonary drug metabolism, clearance, and absorption. In: controlled pulmonary drug delivery, Springer New York, New York, NY, pp 21–50, 2011.

Onoue S, Seto Y, Kato M, Aoki Y, Kojo Y, Yamada S. Inhalable powder formulation of pirfenidone with reduced phototoxic risk for treatment of pulmonary fibrosis. Pharm Res, 2013; 30(6):1586–96.

Pardeshi S, Patil P, Rajput R, Mujumdar A, Naik J. Preparation and characterization of sustained release pirfenidone loaded microparticles for pulmonary drug delivery: spray drying approach. Dry Technol, 2020; 39(3):337–47.

Putri KSS, Ramadhani LS, Rachel T, Suhariyono G, Surini S. Promising chitosan-alginate combination for rifampicin dry powder inhaler to target active and latent tuberculosis. J Appl Pharm Sci, 2022; 12(5):098–103.

Ruwanpura SM, Thomas BJ, Bardin PG. Pirfenidone: Molecular mechanisms and potential clinical applications in lung disease. Am J Respir Cell Mol Biol, 2020; 62(4):413–22.

Sayes CM, Reed KL, Warheit DB. Assessing toxicity of fine and nanoparticles: comparing *in vitro* measurements to *in vivo* pulmonary toxicity profiles. Toxicol Sci, 2007; 97(1):163–80.

Sayf AA. Idiopathic pulmonary fibrosis (IPF) medication. 2021. [Online]. Available via https://emedicine.medscape.com/article/301226-medication (Accessed 23 February 2021).

Shahin HI, Vinjamuri BP, Mahmoud AA, Shamma RN, Mansour SM, Ammar HO, Ghorab MM, Chougule MB, Chablani L. Design and evaluation of novel inhalable sildenafil citrate spray-dried microparticles for pulmonary arterial hypertension. J Control Release, 2019; 302:126–39.

Shahin H, Vinjamuri BP, Mahmoud AA, Mansour SM, Chougule MB, Chablani L. Formulation and optimization of sildenafil citrate-loaded PLGA large porous microparticles using spray freeze-drying technique: a factorial design and *in-vivo* pharmacokinetic study. Int J Pharm, 2021; 597:120320.

She, YX, Yu, QY, Tang, XX. Role of interleukins in the pathogenesis of pulmonary fibrosis. Cell Death Discovery, 2021; 7(1):52.

Simon A, Amaro MI, Cabral LM, Healy AM, De Sousa VP. Development of a novel dry powder inhalation formulation for the delivery of rivastigmine hydrogen tartrate. Int J Pharm, 2016; 501(1–2):124–38.

Spagnolo P, Kropski JA, Jones MG, Lee JS, Rossi G, Karampitsakos T, Maher TM, Tzouvelekis A, Ryerson CJ. Idiopathic pulmonary fibrosis: disease mechanisms and drug development. Pharmacol Ther, 2021; 222:107798

Surini, S, Anggriani, V, Anwar, E. Study of mucoadhesive microspheres based on pregelatinized cassava starch succinate as a new carrier for drug delivery. J Med Sci, 2009; 9(6):249–56.

Surini S, Azzahrah FU, Ramadon D. Microencapsulation of grape seed oil (*Vitis vinifera* L.) with gum arabic as a coating polymer by crosslinking emulsification method. Int J Appl Pharm, 2018; 10(6):194–8.

Surini S, Khotima NH. Stability study of ethylcellulose coated-tocotrienol microcapsules prepared by solvent evaporation and spray drying techniques. Int J Appl Pharm, 2020; 12(Special Issue 1):197–201.

Surini S, Providya R, Putri KSS. Formula optimization of rifampicin dry powder inhalation with chitosan-xanthan carrier using response surface methodology. J Appl Pharm Sci, 2019; 9(1):33–41.

Tabata Y, Ikada Y. Effect of the size and surface charge of polymer microspheres on their phagocytosis by macrophage. Biomaterials, 1988; 9(4):356–62.

Ungaro F, Giovino C, Coletta C, Sorrentino R, Miro A, Quaglia F. Engineering gas-foamed large porous particles for efficient local delivery of macromolecules to the lung. Eur J Pharma Sci, 2010; 41(1):60–70.

Wang X, Wan W, Lu J, Quan G, Pan X, Liu P. Effects of L-leucine on the properties of spray-dried swellable microparticles with wrinkled surfaces for inhalation therapy of pulmonary fibrosis. Int J Pharm, 2021; 610:1–12.

Xu E-Y, Guo J, Xu Y, Li H, Seville PC. Influence of excipients on spray-dried powders for inhalation. Powder Technol, 2014; 256:217–3.

Yoshida H, Usui A, Abe Y, Goda Y, Izutsu K. Relationship between geometric and aerodynamic particle size distributions in the formulation of solution and suspension metered-dose inhalers. AAPS Pharm Sci Tech, 2020; 21(5):158.

How to cite this article:
Hasyyati US, Surini S, Suhariyono G. Prospective pulmonary drug delivery system of pirfenidone microparticles for pulmonary fibrosis. J Appl Pharm Sci, 2023; 13(09):095–105.